Results in Physics 21 (2021) 103536

Contents lists available at ScienceDirect

Results in Physics

journal homepage: www.elsevier.com/locate/rinp

Non-classical computing problems: Toward novel type of quantum computing problems

Mohammed Zidan [a,b,*], Hichem Eleuch [c,d], Mahmoud Abdel-Aty [e]

[a] Faculty of Engineering, King Salman International University, South Sinai, Egypt
[b] College of Engineering, Abu Dhabi University, Abu Dhabi, United Arab Emirates
[c] Department of Applied Physics and Astronomy, University of Sharjah, Sharjah, United Arab Emirates
[d] Department of Applied Sciences and Mathematics, College of Arts and Sciences, Abu Dhabi University, Abu Dhabi, United Arab Emirates
[e] Department of Mathematics, Faculty of Science, Sohag University, Sohag, Egypt

ARTICLE INFO

Keywords:
Deutch's problem
Entanglement measurement
Concurrence

ABSTRACT

Quantum teleportation draws our attention to propose a new type of problems which can not be solved using classical computers. In this paper, we propose one of these problems. Concretely, this paper extends the definition of Deutsch's problem to decide whether a black box U_f applied on a given unknown qubit $\alpha|0\rangle + \beta|1\rangle$, such that $|\alpha| > 0,\ |\beta| > 0,\ and\ |\alpha| \neq |\beta|$, is constant or balanced Boolean function, besides, estimation of $|\alpha|$ and $|\beta|$. Although, this problem is very simple but it can not be solved using classical computers, because qubit can not be implemented physically using classical computers. A novel quantum algorithm based on principle of entanglement measure is proposed to solve this problem. IBMs 5-qubit quantum computer (ibmqx4) is used to realize the proposed algorithm experimentally.

Introduction

The quest to develop quantum algorithms became of an utmost necessity to solve problems with high-cost solving time using classical computers. The superposition and quantum correlation of microscopic systems lead to unique features and capabilities [1–12] compared with macroscopic systems which usually act according to Newtonian mechanics. Entanglement [13–20] is a type of quantum correlation that appears if two quantum systems or more cannot be described independently, even when theyre disjointed by distance [21–25]. Entanglement phenomenon is a crucial resource in quantum computation [21], and its puzzling aspect is a characteristic property of quantum mechanics which was first pointed out by Einstein, Podolsky, and Rosen in their seminal paper [22]. Entanglement offers a unique resource to perform several previously impossible operations such as quantum teleportation [26,27]. Since the degree of entanglement is not plainly quantified, Wootters [28] proposed concurrence measurement that measures the degree of entanglement between two-body systems. Concurrence has been utilized for solving several quantum computing problems (see e.g., [29] and references therein).

In 1985, Deutsch presented the first algorithm that demonstrated how fast quantum algorithms can be in comparison with classical algorithms [30]. A set of quantum algorithms have been proposed since then which solve well-known intractable problems significantly faster than conventional algorithms [31–34].

Quantum computers perform computations via one or more qubits through quantum circuits [21]. Unlike classical bits, qubits follow the two unique properties of quantum mechanics, namely superposition and entanglement. Moreover, teleportation becomes a source of quantum information, where the teleported quantum state is unknown in advance for both the sender and the receiver [35,36]. Recently, teleportation of a quantum gate between two unknown qubits is realized experimentally [37]. Thus, quantum information becomes a more general form of information rather than classical information in classical computers. Consequently, quantum algorithms are needed not only to perform calculations faster on the quantum computers but to perform computations on quantum information too. Recently, K. Nagata et al. they claimed that they proposed an algorithm that uses a single measurement for determination the phase that can be used to differentiate between the functions $f_0, f_1, f_2, and f_3$; as a generalization of Deutsch' algorithm. Nevertheless, they did not explained how their algorithm can do that. So their paper [38] can not be considered as a generalization for Deutsch' algorithm.

In this paper, we go further from speed up solving classical problems

* Corresponding author.
E-mail addresses: mzidan@zewailcity.edu.eg, comsi2014@gmail.com (M. Zidan).

https://doi.org/10.1016/j.rinp.2020.103536
Received 22 September 2020; Accepted 20 October 2020
Available online 3 November 2020

by quantum computing to solving some problems which are intractable to be solved using classical computing. This paper proposes one of these problems which can not be solved using classical computers. Concretely, this paper extends the definition of Deutsch's problem to decide whether a black box U_f applied on a given unknown qubit $\alpha|0\rangle + \beta|1\rangle$, such that $|\alpha| > 0, |\beta| > 0, and |\alpha| \neq |\beta|$, is constant or balanced Boolean function, besides, estimation of $|\alpha|$ and $|\beta|$. Although, this problem is very simple, however it can not be solved using classical computers because unknown qubits cannot be implemented physically on classical computers compared with Deutsch's algorithm that can be simulated on classical computers with more computational effort. Then, we propose a novel algorithm based on concurrence measure to solve the proposed problem. In addition, the analysis of the proposed algorithm is demonstrated theoretically and proved experimentally using quantum state tomography. furthermore, the proposed algorithm is realized empirically on IBMs 5-qubit quantum computer with reliable fidelities.

In Section "Standard Deutsch's problem", we briefly review the standard Deutsch algorithm. Section "Problem statement" explains the problem definition. Sectin "Problem statement" shows the proposed problem. In Section "Concurrence measurement", we briefly describe the techniques used in the proposed algorithm and the proposed application. Section "The proposed algorithm and analysis" presents a full description of the proposed algorithm that solves the problem and its analysis. In Section "Error estimation", the error estimation of the proposed algorithm is investigated in Section. In Section "Experimental realization of the proposed algorithm using IBM's quantum computer", the full realization of the proposed algorithm using IBM's quantum computer, is implemented. Finally, conclusions are drawn in Section "Conclusion".

Standard Deutsch's problem

David Deutsch is one of the pillars of quantum computing algorithms. He proposed the first problem that can be solved quantum mechanically faster than classical algorithms do [30,31]. This problem was defined as follows:

Given: A black-box for computing an unknown function $f : \{0,1\} \to \{0,1\}$.

Goal: Determine whether $f(0) = f(1)$ or not, by a single query to f. In other words, the given orcale represents a function that takes one of the following cases:

$$f(x) = \begin{cases} f(0) = f(1), \\ or\ f(0) \neq f(1). \end{cases} \tag{1}$$

Classically, there are two queries for f must be conducted to determine if $f(0) = f(1)$. Deutsch proposed the algorithm that harnesses quantum parallelism and interference to solve this query deterministically by calling an oracle U_f only once. The required steps of Deutsch's algorithm are:

1. Initializing the two qubits register $|\phi_0\rangle$ as follows
   $$|\phi_0\rangle = |0\rangle|1\rangle.$$
2. Applying Hadamard-gate H on each qubit
   $$|\phi_1\rangle = H^{\otimes 2}|\phi_0\rangle.$$
3. Evolving the system by U_f operator
   $$|\phi_2\rangle = U_f|\phi_1\rangle,$$
   where the action of U_f is $U_f|x\rangle|y\rangle \to |x\rangle|y \oplus f(x)\rangle$.
4. Applying Hadamard-gate H on the first qubit
   $$|\phi_3\rangle = (H \otimes I)|\phi_2\rangle,$$
   where I is the identity operator.
5. Measuring the first qubit
   (i) If the post-measurement state of the first qubit is 0 then
   $$f(0) = f(1).$$
   (ii) If the post-measurement state of the first qubit is 1 then
   $$f(0) \neq f(1).$$

Problem Statement

For unknown black box U_f which encodes some univariate Boolean function and applied on a given unknown qubit $|t\rangle$, it is required to check the applied function is constant or balanced. The abstract problem is described as follows:

Given: (i) An unknown qubit $|t\rangle = \alpha|0\rangle + \beta|1\rangle$ *in a pure state*, such that $|\alpha\rangle > 0$, $|\beta\rangle > 0$, *and* $|\alpha\rangle \neq |\beta\rangle$.
(ii) An Orcale U_f represents an unknown Boolean function $f : \{0, 1\} \to \{0,1\}$is applied on $|t\rangle$.

Goal: (i) Classify U_f into one of two classes: Constant function or balanced function.
(ii) Estimate $|\alpha_\epsilon|$ *and* $|\beta_\epsilon|$ *for the given unknown qubit* $|t|$ *such that*: $(1-\epsilon)|\alpha_\epsilon| \leqslant |\alpha_\epsilon| \leqslant (1+\epsilon)|\alpha_\epsilon|, and (1-\epsilon)|\beta_\epsilon| \leqslant |\beta_\epsilon| \leqslant (1+\epsilon)|\beta_\epsilon|$.

Remark. If $|\alpha| = 0$, or $|\beta| = 0$, then the proposed problem is converted from quantum problem to standard Deutsch's problem and can be solved by Deutsch's algorithm, because the problem is converted from quantum problem to classical problem.

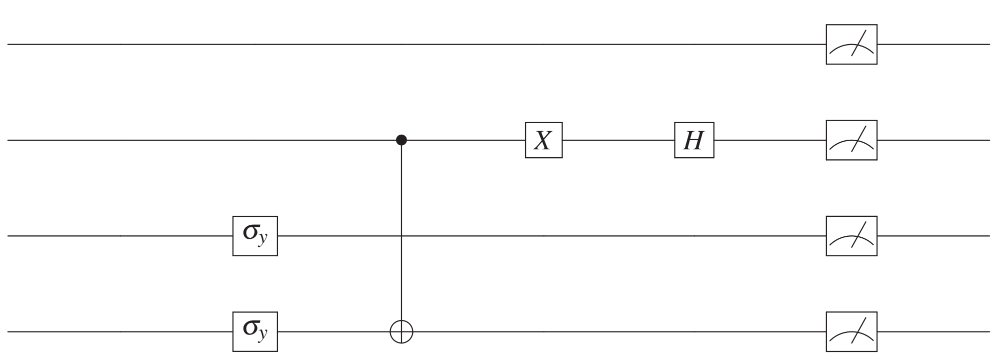

Fig. 1. The circuit model of Romero et al. protocol [45].

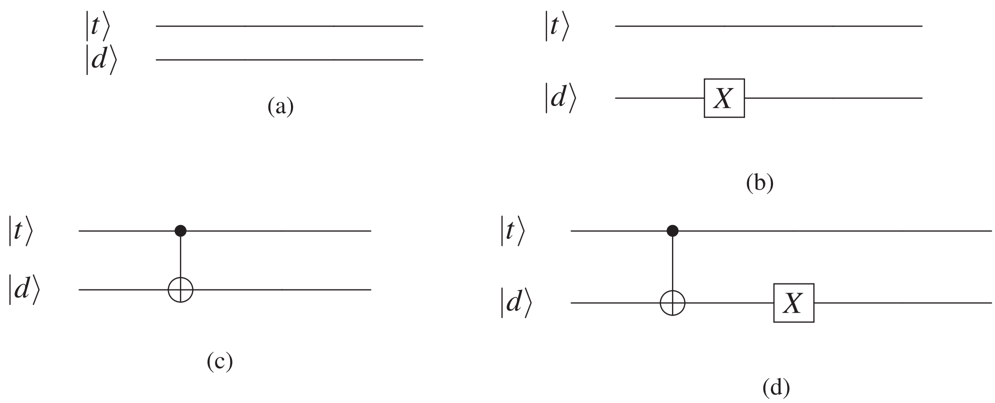

Fig. 2. The circuit model for the four possible univariate Boolean functions applied on unknown qubit $|t\rangle = \alpha|0\rangle + \beta|1\rangle$. (a) Case-1: constant function f_0; (b) Case-2: constant function f_1; (c) Case-3: balanced function f_2; (d) Case-4: balanced function f_3.

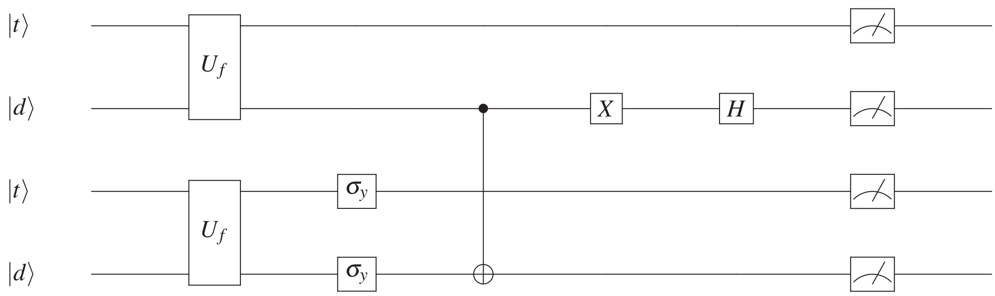

Fig. 3. Quantum circuits of the operator D is realized by Romero et al. protocol [45] by feeding it with a two decoupled copies.

Concurrence measure

An arbitrary composite system of two-qubit described by a state $|\chi\rangle$ is called two-qubit entangled system if and only if it cannot always be written mathematically in the product form $|\chi\rangle \neq |\chi_1\rangle \otimes |\chi_2\rangle$. Although this mathematical definition is simple but it can not quantify the degree of entanglement in a two-qubit system [39,40]. Wootters [28] proposed concurrence as a measurement of the degree of entanglement between arbitrary two-body systems.

Consider an arbitrary two-qubit system in a pure state described as

$$|\alpha\rangle = d_0\ |00\rangle + d_1\ |01\rangle + d_2\ |10\rangle + d_3\ |11\rangle, \tag{2}$$

where $\sum_{i=0}^{3}|d_i|^2 = 1$. Consider can be calculated as follows:

$$C(\ |\alpha\rangle) = |\ \langle\chi|\sigma_y \otimes \sigma_y|\chi^{\dagger}\rangle\ |, \tag{3}$$

where $\sigma_y = i|1\rangle\langle 0| - i|0\rangle\langle 1|$, and $i = \sqrt{-1}$. According to Eq. (3) concurrence can be expressed as

$$C(\ |\ \alpha\ |\ ) = 2\ |d_0 d_3 - d_1 d_2\ |. \tag{4}$$

Concurrence C is bounded in the interval $[0,1]$, when $C = 1$, the state is called maximally entangled state, e.g., Bell states. And if $C = 0$, the state is called separable state; otherwise the state is called weakly entangled state.

Researchers proposed several approaches to realize Eq. (4) experimentally. Their concepts are based on a linear optical system, nonlinear optical system and atomic levels have been proposed [41–43,39,44–46,44,47–51,45] by using collective sharp measurements with simultaneous copies of the desired state. Recently, Tukiainen et al. [52] developed a procedure to quantify the concurrence of an arbitrary two-qubit via weak measurement. It is applicable for all two-qubit systems without requiring simultaneous copies of the desired state [52]. So far, it is apparent that realizing Eq. (4) is still under continuous investigation and open research direction especially if the weak measurement is considered [53,52]. Therefore, to use concurrence as an entanglement measurement operator, this paper considers it as a black-box operator that can be defined according to the following definition.

Definition. For an arbitrary two-qubit system in a pure state, a black-box D is a measuring operator that measures the concurrence between those qubits.

This definition is used in step 3 in the proposed algorithm (see Section 'The proposed algorithm'). It is employed to distinguish between constant and balanced functions in the general form. On the other hand, the D operator will be implemented using Romero et al. circuit [45] in order to realizing the proposed algorithm using IBM's quantum computer.

Concurrence measure realization

Romero et al. [45], proposed a protocol based on quantum mechanics postulates to measure the concurrence of a two-qubit pure state $|\chi\rangle$ directly. The circuit model of this protocol is depicted in Fig. 1. The steps of this protocol are summarized as follows:

1. Register Preparation: append two decoupled copies of the designated state $|\chi\rangle$ as $|\zeta_0\rangle = |\chi\rangle \otimes |\chi\rangle$.
2. $|\zeta_1\rangle = (I^{\otimes 2} \otimes \sigma_y \otimes \sigma_y)|\zeta_0\rangle$, where I is the 2×2 identity operator.
3. $|\zeta_2\rangle = CNOT_{\zeta_{1_2},\zeta_{1_4}}|\zeta_1\rangle$.
   In this step $CNOT$ is applied on the second and fourth qubits as the control and the target qubits, respectively, to xor those qubits as $CNOT|\zeta_{1_2},\zeta_{1_4}\rangle = |\zeta_{1_2},\zeta_{1_2} \oplus \zeta_{1_4}\rangle$.
4. $|\zeta_3\rangle = (I \otimes X \otimes I^{\otimes 2})|\zeta_2\rangle$, where X is the Not-gate $X = |0\rangle\langle 1| + |1\rangle\langle 0|$.
5. $|\zeta_4\rangle = (I \otimes H \otimes I^{\otimes 2})|\zeta_3\rangle$.
   Therefore, the state of the overall system can be computed as

$$|\zeta_4\rangle = \frac{1}{\sqrt{2}}\{(d_1d_2 - d_0d_3)|0000\rangle + (d_0d_2 - d_1d_3)|0001\rangle + (d_1^2 - d_0^2)|0011\rangle + (d_1d_2 + d_0d_3)|0100\rangle - (d_0d_2 + d_1d_3)|0101\rangle - 2d_0d_1|0110\rangle + (d_1^2 + d_0^2)|0111\rangle$$
$$- (d_2^2 + d_3^2)|1101\rangle + (d_2^2 - d_3^2)|1001\rangle + (d_1d_2 - d_0d_3)|1010\rangle - (d_0d_2 - d_1d_3)|1011\rangle + 2d_2d_3|1100\rangle - (d_1d_2 + d_0d_3)|1110\rangle + (d_0d_2 + d_1d_3)|1111\rangle\}. \quad (5)$$

Comparing Eq. (4) and Eq. (5) yields that the concurrence of state $|\chi\rangle$ is implemented in the coefficient $(d_1d_2 - d_0d_3)$ in Eq. (5). Thus, after measuring the state of the four qubits, the concurrence can be given as follows:

$$C(|\chi\rangle) = 2\sqrt{2P_{0000}} \quad or \quad C(|\chi\rangle) = 2\sqrt{2P_{1010}}. \quad (6)$$

G. Romero et al. proposed to use atoms crossing three-dimensional

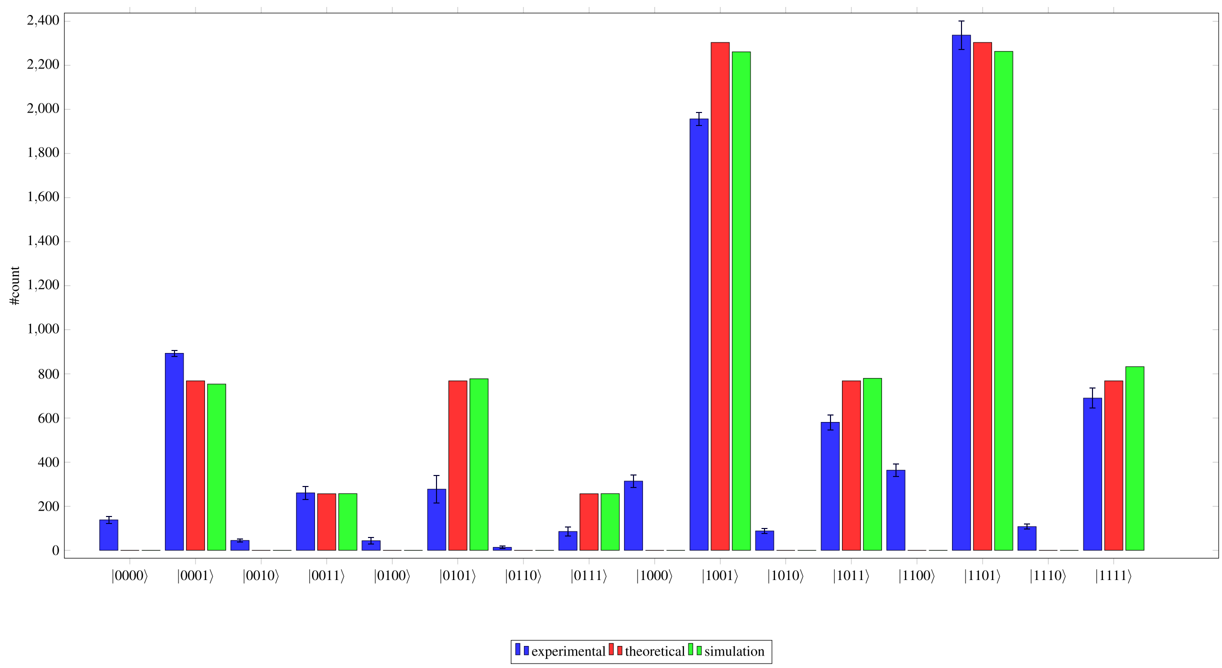

Fig. 4. f_0 for state $|t\rangle = \sqrt{\frac{1}{4}}|0\rangle + \sqrt{\frac{3}{4}}|1\rangle$.

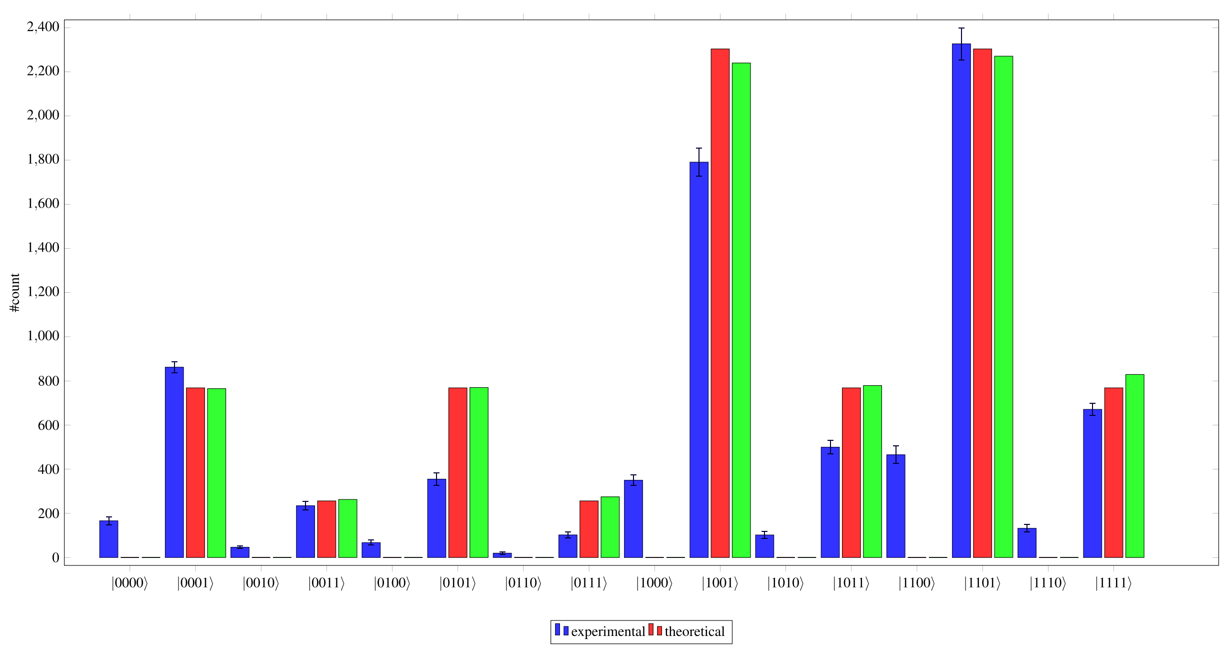

Fig. 5. f_1 for state $|t\rangle = \sqrt{\frac{1}{4}}|0\rangle + \sqrt{\frac{3}{4}}|1\rangle$. (a) concurrence; (b) Measuring qubit $|t\rangle$.

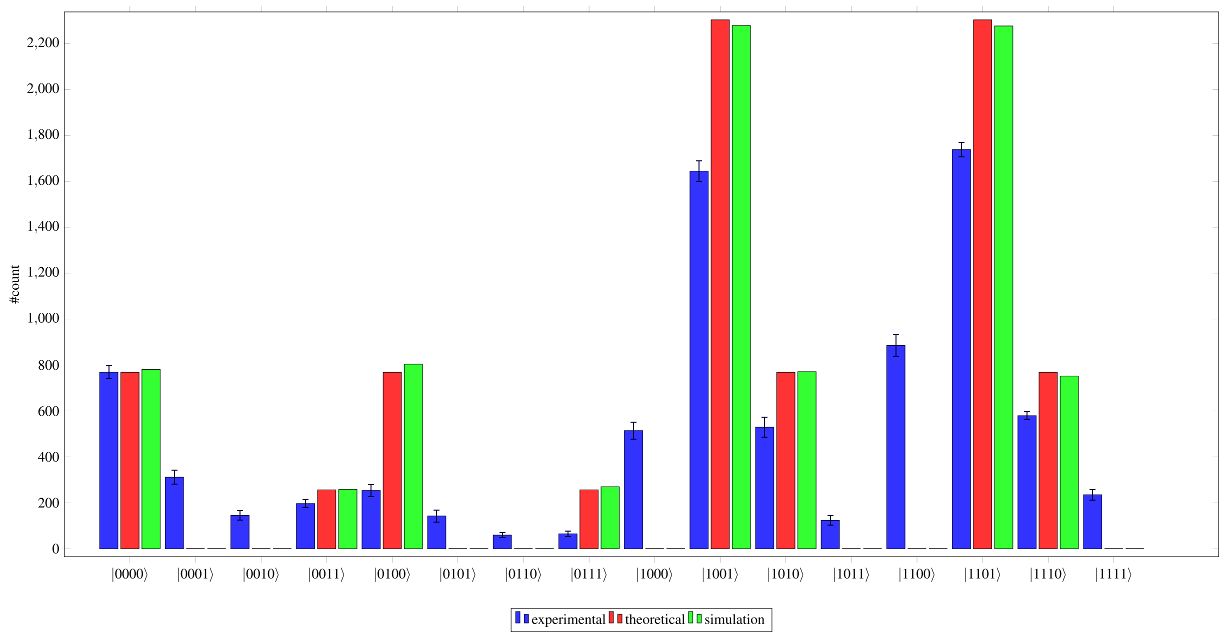

Fig. 6. f_2 for state $|t\rangle = \sqrt{\frac{1}{4}}|0\rangle + \sqrt{\frac{3}{4}}|1\rangle$. (a) concurrence; (b) Measuring qubit $|t\rangle$.

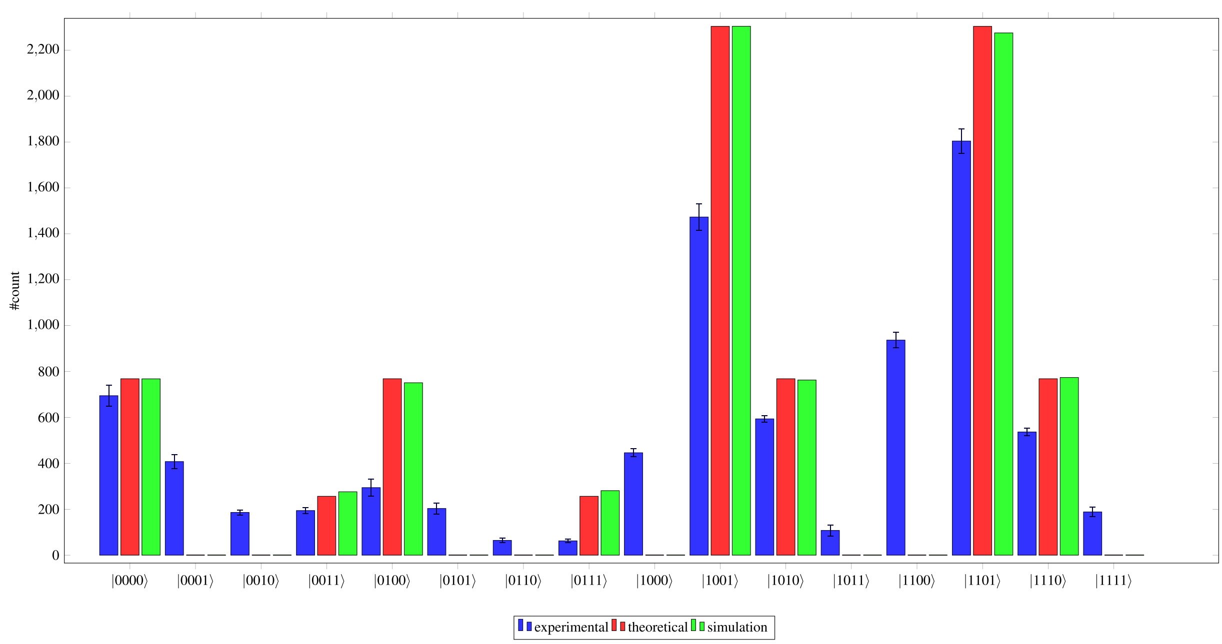

Fig. 7. f_3 for state $|t\rangle = \sqrt{\frac{1}{4}}|0\rangle + \sqrt{\frac{3}{4}}|1\rangle$.

microwave cavities or trapped ion systems as two different possible scenarios to realize this protocol [45]. In this paper, this protocol is realized experimentally using IBM's five-qubit quantum computer as one of the possible structures for operator D toward the realization of the proposed algorithm.

The proposed algorithm and analysis

The proposed algorithm utilizes the principle of quantum parallelism, interference, and concurrence which are the power of quantum mechanics to solve the problem mentioned in Section "Problem statement".

The proposed algorithm

1. Register Preparation: Given an unknown $|t\rangle = \alpha|0\rangle + \beta|1\rangle$ in a pure state, attach a single ancilla qubit $|d\rangle$ initialized in the vacuum state $|0\rangle$ as follows:

$$|\psi_0\rangle = |t\rangle \otimes |d\rangle = \alpha|00\rangle + \beta|10\rangle.$$

2. Apply the oracle U_f

$$|\psi_1\rangle = U_f|\psi_0\rangle = \alpha|0, 0 \oplus f(0)\rangle + \beta|1, 0 \oplus f(1)\rangle.$$

3. Repeat Step 1 and Step 2 to obtain another copy of the state $|\psi_1\rangle$.

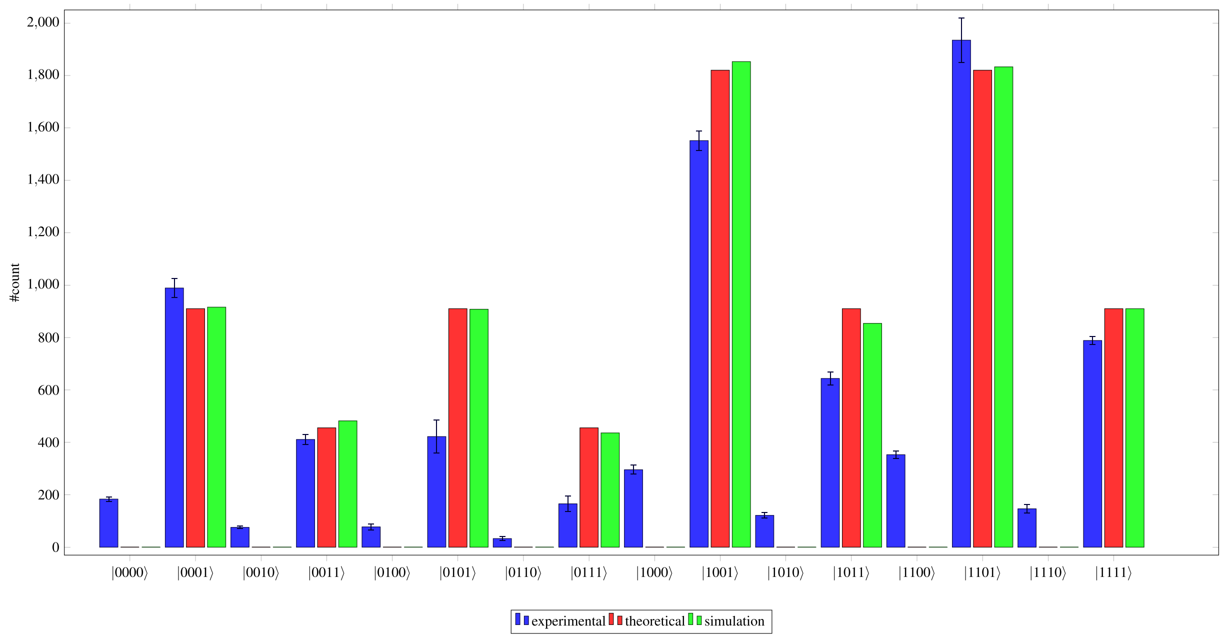

Fig. 8. f_0 for state $|t\rangle = \sqrt{\frac{1}{3}}|0\rangle + \sqrt{\frac{2}{3}}|1\rangle$.

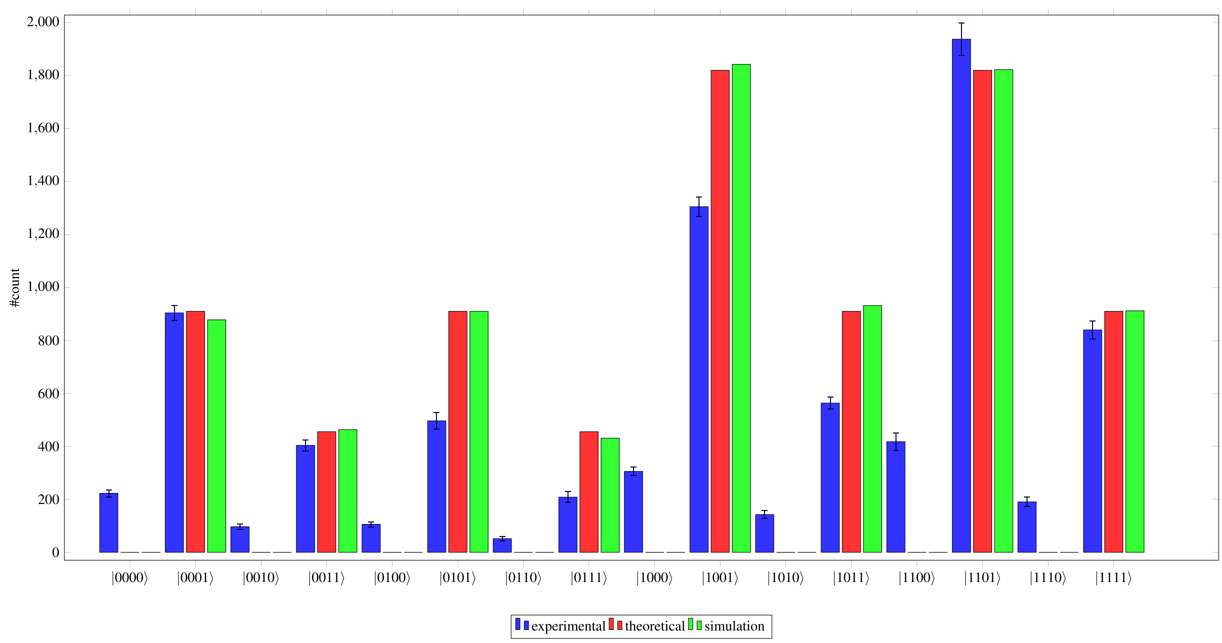

Fig. 9. f_1 for state $|t\rangle = \sqrt{\frac{1}{3}}|0\rangle + \sqrt{\frac{2}{3}}|1\rangle$. (a) concurrence; (b) Measuring qubit $|t\rangle$.

4. Apply the device D, the circuit shown in Fig. 1, on the two copies of the state $|\psi_1\rangle$. Then estimate the probabilities of the states $|0000\rangle, |1010\rangle, |0011\rangle, |0111\rangle, |1001\rangle$ and $|1101\rangle$.

   Estimate the concurrence value C using Eq. (19).

   If $C = 0$then the applied function is constant function $f(0) = f(1)$.

   If $C > 0$ then the applied function is balanced function $f(0) \neq f(1)$.

   Estimate $|\alpha|$ using one of the formulas of $|\alpha| = \sqrt[4]{2P_{0011}} or |\alpha| = \sqrt[4]{2P_{0111}}$, and $|\beta| = \sqrt{1-\alpha^2}$.

Analysis of performance

1. In step 1, the quantum system is initialized by appending an ancila qubit $|d\rangle$ in state $|0\rangle$ to the unknown qubit $|t\rangle$.
2. In step 2, the given black box U_f is applied between the qubits $|t\rangle$ and $|d\rangle$ as $U_f|t\rangle|d\rangle \rightarrow |t\rangle|d \oplus f(t)\rangle$. Performance of the proposed algorithm for each case is investigated individually as follows:
   - In the case $f(0) = f(1)$, constant function, then there are two possibilities which are:
     (a) Either the given black-box is the Boolean function $U_f = f_0$ for which $f(0) = f(1) = 0$, then U_f evolves the state of $|td\rangle$ as:

$$|td\rangle = \alpha|0, 0 \oplus 0\rangle + \beta|1, 0 \oplus 0\rangle = (\alpha|0\rangle + \beta|1\rangle)|0\rangle. \tag{7}$$

Thus this oracle does not produce a measurable entanglement between $|t\rangle$ and $|d\rangle$ qubits because it is separable state. Then, the concurrence between those qubits is vanished, $C = 0$, when measured via operator D in step 3. Meanwhile, in this case the state of $|d\rangle$ collapses deterministically to state $|0\rangle$.

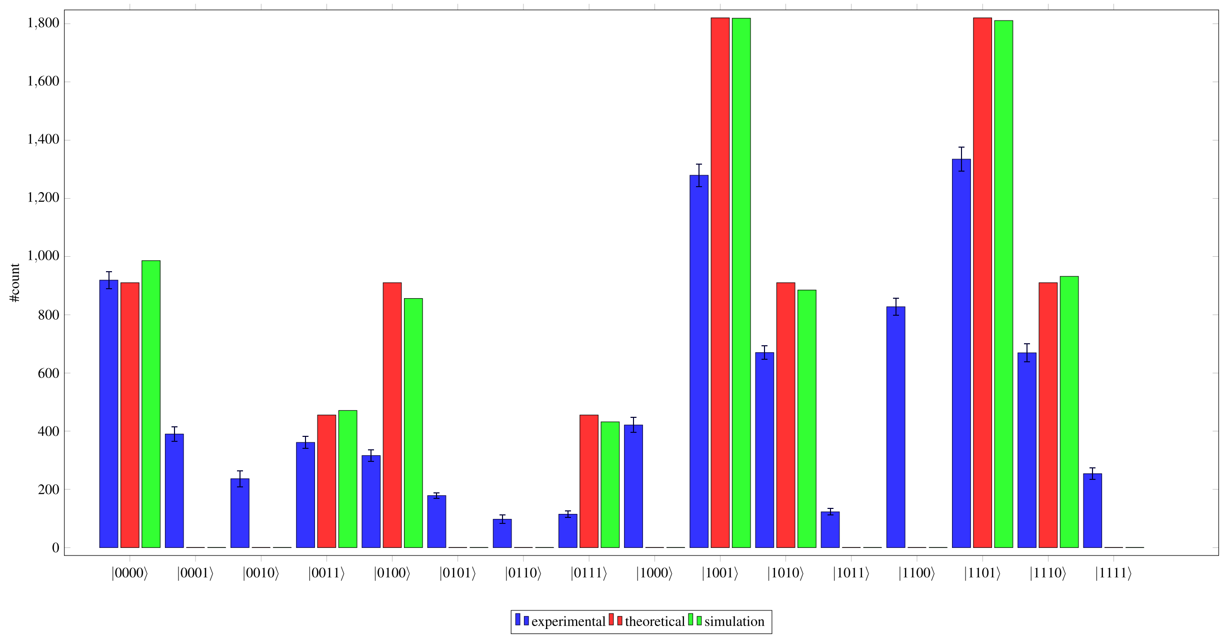

Fig. 10. f_2 for state $|t\rangle = \sqrt{\frac{1}{3}}|0\rangle + \sqrt{\frac{2}{3}}|1\rangle$. (a) concurrence; (b) Measuring qubit $|t\rangle$.

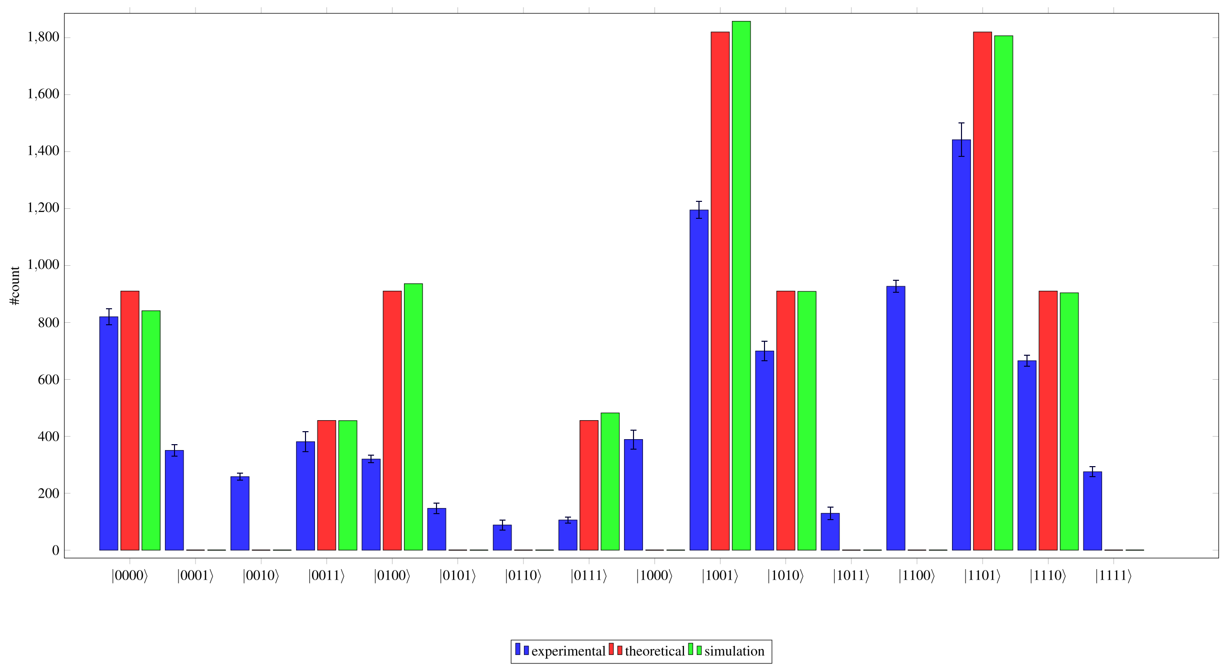

Fig. 11. f_3 for state $|t\rangle = \sqrt{\frac{1}{3}}|0\rangle + \sqrt{\frac{2}{3}}|1\rangle$. (a) concurrence; (b) Measuring qubit $|t\rangle$.

By comparing Eq. (4) and Eq. (7), we obtain that

$$d_0 = \alpha,\ d_1 = 0,\ d_2 = \beta,\ \text{and}\ d_3 = 0. \tag{8}$$

From Eq. (8) and Eq. (5), we obtain that

$$|\zeta_4\rangle = \frac{1}{\sqrt{2}}\{\alpha\beta|0001\rangle - \alpha^2|0011\rangle - \alpha\beta|0101\rangle + \alpha^2|0111\rangle - \beta^2|1101\rangle + \beta^2|1001\rangle - \alpha\beta|1011\rangle + \alpha\beta|1111\rangle\}. \tag{9}$$

(b) Or the given black-box is the Boolean function $U_f = f_1$ for which $f(0) = f(1) = 1$, then U_f evolves the state of $|td\rangle$ as:

$$|td\rangle = \alpha|0, 0 \oplus 1\rangle + \beta|1, 0 \oplus 1\rangle = (\alpha|0\rangle + \beta|1\rangle)|1\rangle. \tag{10}$$

Also, the Oracle in this case does not produce a measurable entanglement between $|t\rangle$ and $|d\rangle$ because it is a separable state. Then concurrence between those qubits is $C = 0$, when measured via operator D in step 3. Meanwhile, in this case, the state of $|d\rangle$ collapses deterministically to state $|1\rangle$. By comparing Eq. (4) and Eq. (10), we obtain that

$$d_0 = 0,\ d_1 = \alpha,\ d_2 = 0,\ \text{and}\ d_3 = \beta. \tag{11}$$

From Eqs. (11) and (5), we obtain that

$$|\zeta_4\rangle = \frac{1}{\sqrt{2}}\{-\alpha\beta|0001\rangle + \alpha^2|0011\rangle - \alpha\beta|0101\rangle + \alpha^2|0111\rangle - \beta^2|1101\rangle$$
$$-\beta^2|1001\rangle + \alpha\beta|1011\rangle + \alpha\beta|1111\rangle\}. \quad (12)$$

- On the other hand, if $f(0) \neq f(1)$ then there are two possibilities which are:
  c) Either the given black-box is the Boolean function $U_f = f_2$ for which $f(0) = 0, f(1) = 1$, then U_f evolves the state of $|td\rangle$ as:

$$|td\rangle = \alpha|0, 0\oplus 0\rangle + \beta|1, 0\oplus 1\rangle = \alpha|00\rangle + \beta|11\rangle. \quad (13)$$

This is a two-qubit entangled system of $|t\rangle$ and $|d\rangle$. So, the concurrence between those qubits is non-zero $C > 0$ when measured via operator D in step 3. Consequently, the state of $|td\rangle$ always collapses to state $|00\rangle$ or to state $|11\rangle$.

By comparing Eqs. (4) and (13), we obtain that

$$d_0 = \alpha,\ d_1 = 0,\ d_2 = 0,\ \text{and } d_3 = \beta. \quad (14)$$

From Eq. (14) and Eq. (5), we obtain that

$$|\zeta_4\rangle = \frac{1}{\sqrt{2}}\{-\alpha\beta|0000\rangle - \alpha^2|0011\rangle + \alpha\beta|0100\rangle - \alpha^2|0111\rangle - \beta^2|1101\rangle$$
$$-\beta^2|1001\rangle - \alpha\beta|1010\rangle - \alpha\beta|1110\rangle\}. \quad (15)$$

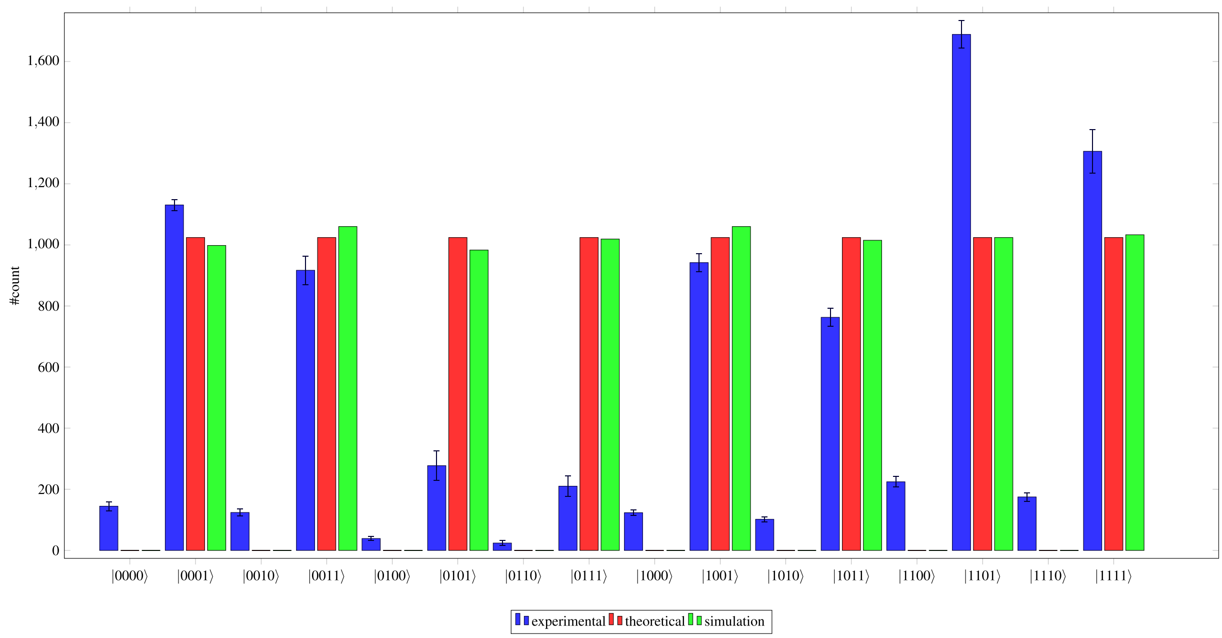

Fig. 12. f_0 for state $|t\rangle = \sqrt{\frac{1}{2}}|0\rangle + \sqrt{\frac{1}{2}}|1\rangle$. (a) concurrence; (b) Measuring qubit $|t\rangle$.

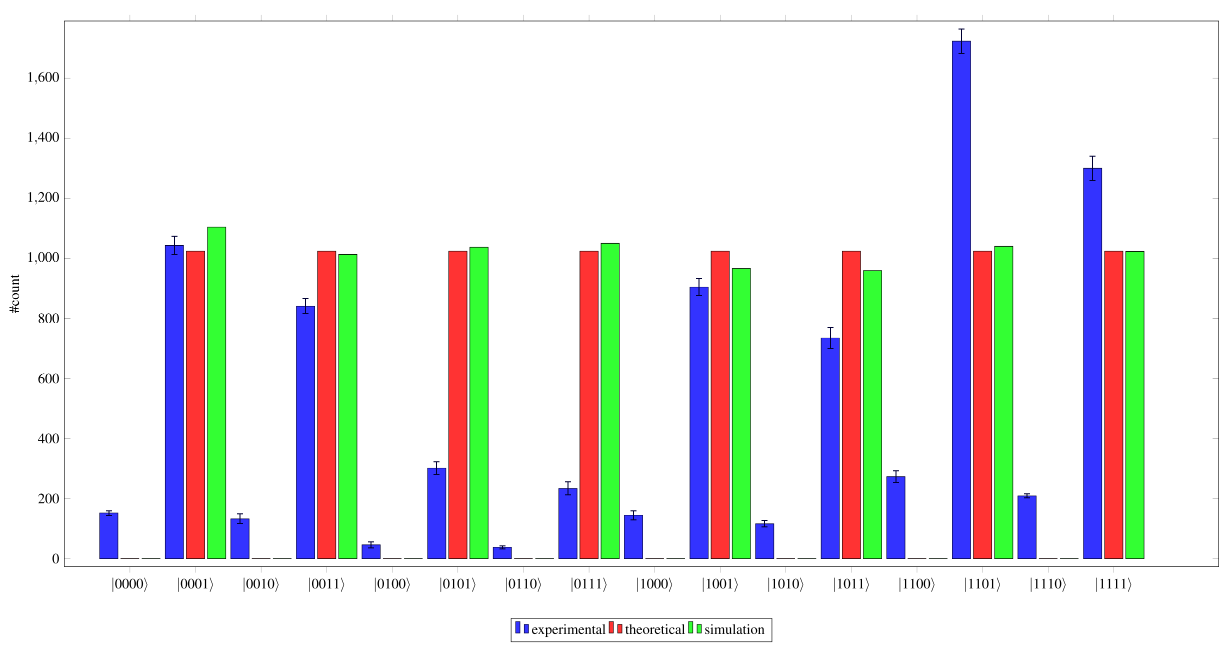

Fig. 13. f_1 for state $|t\rangle = \sqrt{\frac{1}{2}}|0\rangle + \sqrt{\frac{1}{2}}|1\rangle$. (a) concurrence; (b) Measuring qubit $|t\rangle$.

d) Either the given black-box is the Boolean function $U_f = f_3$ for which $f(0) = 1, f(1) = 0$, then U_f evolves the state of $|td\rangle$ as:

$$|td\rangle = |0, 0 \oplus 1\rangle + \beta|1, 0 \oplus 0\rangle = \alpha|01\rangle + \beta|10\rangle. \tag{16}$$

Also, this is a two-qubit entangled system of $|t\rangle$ and $|d\rangle$. So, the concurrence between those qubits is $C > 0$ when measured via operator D in step 3. Consequently, the state of $|td\rangle$ always collapses to state $|01\rangle$ or to state $|10\rangle$.

By comparing Eqs. (4) and (16), we obtain that

$$d_0 = 0, d_1 = \alpha, d_2 = \beta, \text{ and } d_3 = 0. \tag{17}$$

From Eqs. (17) and (5), we obtain that

$$|\zeta_4\rangle = \frac{1}{\sqrt{2}}\{\alpha\beta|0000\rangle + \alpha^2|0011\rangle + \alpha\beta|0100\rangle + \alpha^2|0111\rangle - \beta^2|1101\rangle + \beta^2|1001\rangle + \alpha\beta|1010\rangle - \alpha\beta|1110\rangle\}. \tag{18}$$

Therefore, the concurrence value C is crucial to decide if the applied oracle is one of the two constant functions or is one of the two balanced functions. Eventually, it is clear from Eqs. (9), (12), (15) and (18) that the concurrence value C of the entangled states given by Eqs. (7), (10), (13) and (16) can be estimated as follows:

$$C = \sqrt{2P_s}, \ P_s = P_{0000} + P_{0100} + P_{1010} + P_{1110}, \tag{19}$$

where P_{0000}, P_{0100}, P_{1010}, and P_{1110} are the success probabilities of

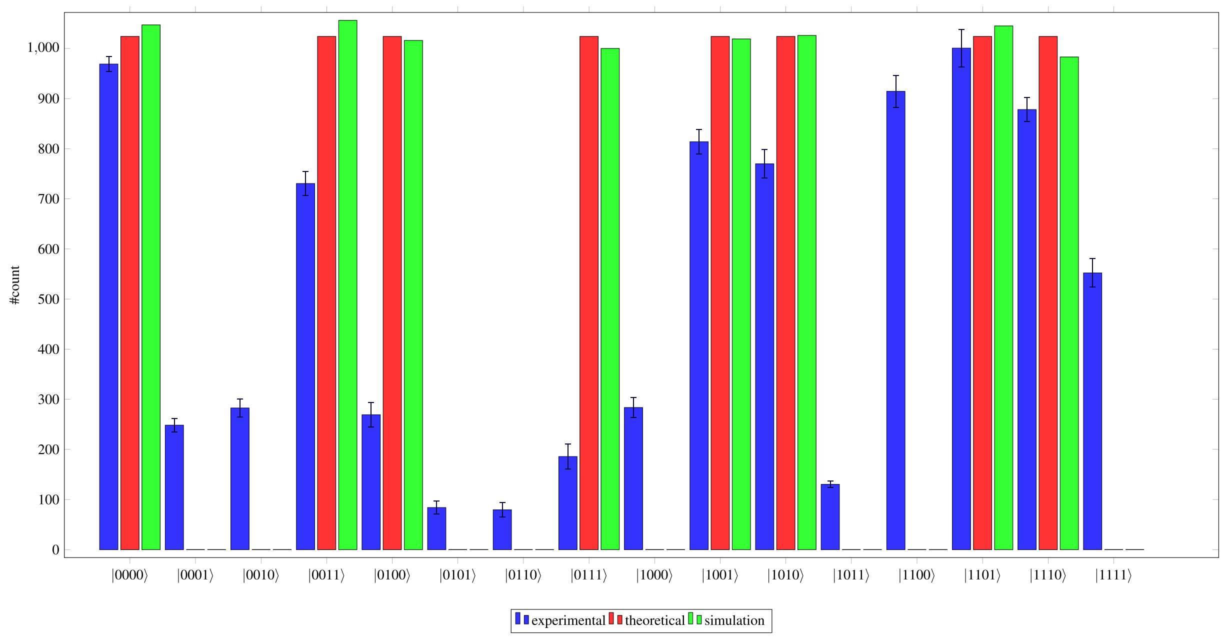

Fig. 14. f_2 for state $|t\rangle = \sqrt{\frac{1}{2}}|0\rangle + \sqrt{\frac{1}{2}}|1\rangle$. (a) concurrence; (b) Measuring qubit $|td\rangle$.

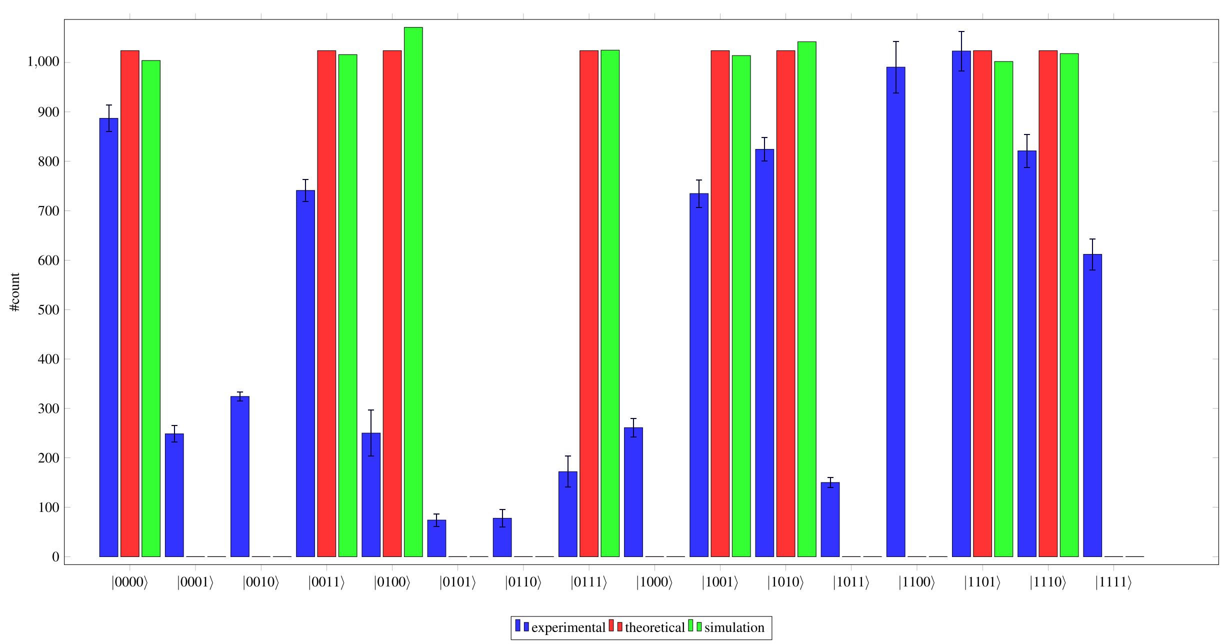

Fig. 15. f_3 for state $|t\rangle = \sqrt{\frac{1}{2}}|0\rangle + \sqrt{\frac{1}{2}}|1\rangle$.

the states $|0000\rangle$, $|0100\rangle$, $|1010\rangle$, and $|1110\rangle$, respectively. Additionally, it is clear from Eqs. (9), (12), (15), (18) that $|\alpha|$ and $|\beta|$ can be estimated as follows:

$$|\alpha| = \sqrt[4]{2P_\alpha}, P_\alpha = P_{0011} + P_{0111}, \text{ and } |\beta| = \sqrt{1 - |\alpha|^2}, \tag{20}$$

where P_{0011}, and P_{0111} are the success probabilities of the states $|0011\rangle$ and $|0111\rangle$, respectively.

Remark:

It worth important to note that, the problem of this paper is solved quantum mechanically only because unknown qubits cannot be implemented physically on classical computers.

Error estimation

Error estimation of the concurrence value C

It is explained in Section 'Analysis of performance' that the degree of entanglement of the entangled states given by Eqs. (7), (10), (13) and (16) can be estimated quantum mechanically using Eq. (19). Thus, the total success probabilities of these states together P_s, from Eqs. (15) and (18), is given by

$$P_s = \frac{4}{2}|\alpha\beta|^2 = 2|\alpha\beta|^2 = \frac{C^2}{2}.$$

The standard deviation of the binomial random variable after one trial is $\sqrt{P_s(1 - P_s)}$. Hence, the standard deviation of the number of obtaining the states $|0000\rangle, |0100\rangle, |1010\rangle, \text{and} |1110\rangle$ is $\sqrt{KP_s(1 - P_s)}$. The probability is accessible by normalizing the number of obtaining the states $|0000\rangle$, $|0100\rangle$, $|1010\rangle$, and $|1110\rangle$ to the total number of measurements trials K. This gives the standard error of measuring P_s as

$$\epsilon_{P_s} = \frac{\sqrt{KP_s(1 - P_s)}}{K}.$$

According to Eq. (19), the concurrence is estimated by $C = \sqrt{2P_s}$, then the standard error of estimation the concurrence value C is calculated by

$$\epsilon_C = \frac{\partial C}{\partial P_s}\epsilon_{P_s} = \sqrt{\frac{(1 - P_s)}{2K}}. \tag{21}$$

Error estimation of $|\alpha|$

The coefficient $|\alpha|$ of the entangled states given by Eqs. (7), (10), (13) and (16) can be estimated by

$$P_\alpha = P_{0011} + P_{0111} = |\alpha|^4.$$

The standard deviation of the binomial random variable after one trial is $\sqrt{P_\alpha(1 - P_\alpha)}$. Hence, the standard deviation of the number of obtaining the states $|0000\rangle$, $|0100\rangle$, $|1010\rangle$, and $|1110\rangle$ is $\sqrt{KP_\alpha(1 - P_\alpha)}$. The probability is accessible by normalizing the number of obtaining the states $|0000\rangle$, $|0100\rangle$, $|1010\rangle$, and $|1110\rangle$ to the total number of measurements trials K. This gives the standard error of measuring P_α as

$$\epsilon_{P_\alpha} = \frac{\sqrt{KP_\alpha(1 - P_\alpha)}}{K}.$$

Where $|\alpha| = (P_\alpha)^{\frac{1}{4}}$, then the standard error of estimation the coefficient $|\alpha|$ is calculated by

$$\epsilon_\alpha = \frac{\partial \alpha}{\partial P_\alpha}\epsilon_{P_\alpha} = \frac{1}{P_\alpha^{\frac{1}{4}}}\sqrt{\frac{(1 - P_\alpha)}{16K}}. \tag{22}$$

Table 1
Statistical fidelities for the circuits implemented using IBM's 5 qubit quantum computer (ibmqx4) for each Boolean function shown in Fig. 2.

$\|t\rangle$	f_0	f_1	f_2	f_3
$\|t\rangle = \sqrt{\frac{1}{4}}\|0\rangle + \sqrt{\frac{3}{4}}\|1\rangle$	0.919899951	0.906680019	0.832028178	0.824411888
$\|t\rangle = \sqrt{\frac{1}{3}}\|0\rangle + \sqrt{\frac{2}{3}}\|1\rangle$	0.908907419	0.894298992	0.821672951	0.81912885
$\|t\rangle = \sqrt{\frac{1}{2}}\|0\rangle + \sqrt{\frac{1}{2}}\|1\rangle$	0.900799072	0.893310447	0.803655017	0.790613395

Table 2
$|t\rangle = \sqrt{\frac{1}{4}}|0\rangle + \sqrt{\frac{3}{4}}|1\rangle.$

U_f	$\|\alpha^{Tho}\|$	$\|\alpha^{Sim}\|$	$\|\alpha^{Real}\|$
f_0	0.5002	0.5005	0.4532
f_1	0.5002	0.5062	0.4503
f_2	0.5002	0.5039	0.4227
f_3	0.5002	0.5106	0.4206

Table 3
$|t\rangle = \sqrt{\frac{1}{3}}|0\rangle + \sqrt{\frac{2}{3}}|1\rangle.$

$\|\alpha\|$	$\|\alpha^{Tho}\|$	$\|\alpha^{Sim}\|$	$\|\alpha^{Real}\|$
f_0	0.5775	0.5786	0.5151
f_1	0.5775	0.5748	0.5228
f_2	0.5775	0.5762	0.4909
f_3	0.5775	0.5816	0.4937

Table 4
$|t\rangle = \sqrt{\frac{1}{2}}|0\rangle + \sqrt{\frac{1}{2}}|1\rangle.$

$\|\alpha\|$	$\|\alpha^{Tho}\|$	$\|\alpha^{Sim}\|$	$\|\alpha^{Real}\|$
f_0	0.7071	0.7098	0.609
f_1	0.7071	0.7084	0.6018
f_2	0.7071	0.7078	0.5783
f_3	0.7071	0.7065	0.5778

Table 5
The experimental architecture of the ibmqx4 qubits.

Qubits	Gate error (10^{-3})	MultiQubit gate error (10^{-2})	Readout error (10^{-2})	Relaxation time $T_1(\mu s)$	Coherence time $T_2(\mu s)$
Q0	0.52	CX_{20}: 2.48	3.90	50.80	56.60
Q1	1.72	CX_{10}: 2.56	6.50	62.00	22.50
Q2	1.12	CX_{32}: 5.33	2.20	43.00	43.60
Q3	1.63	–	1.40	56.10	26.30

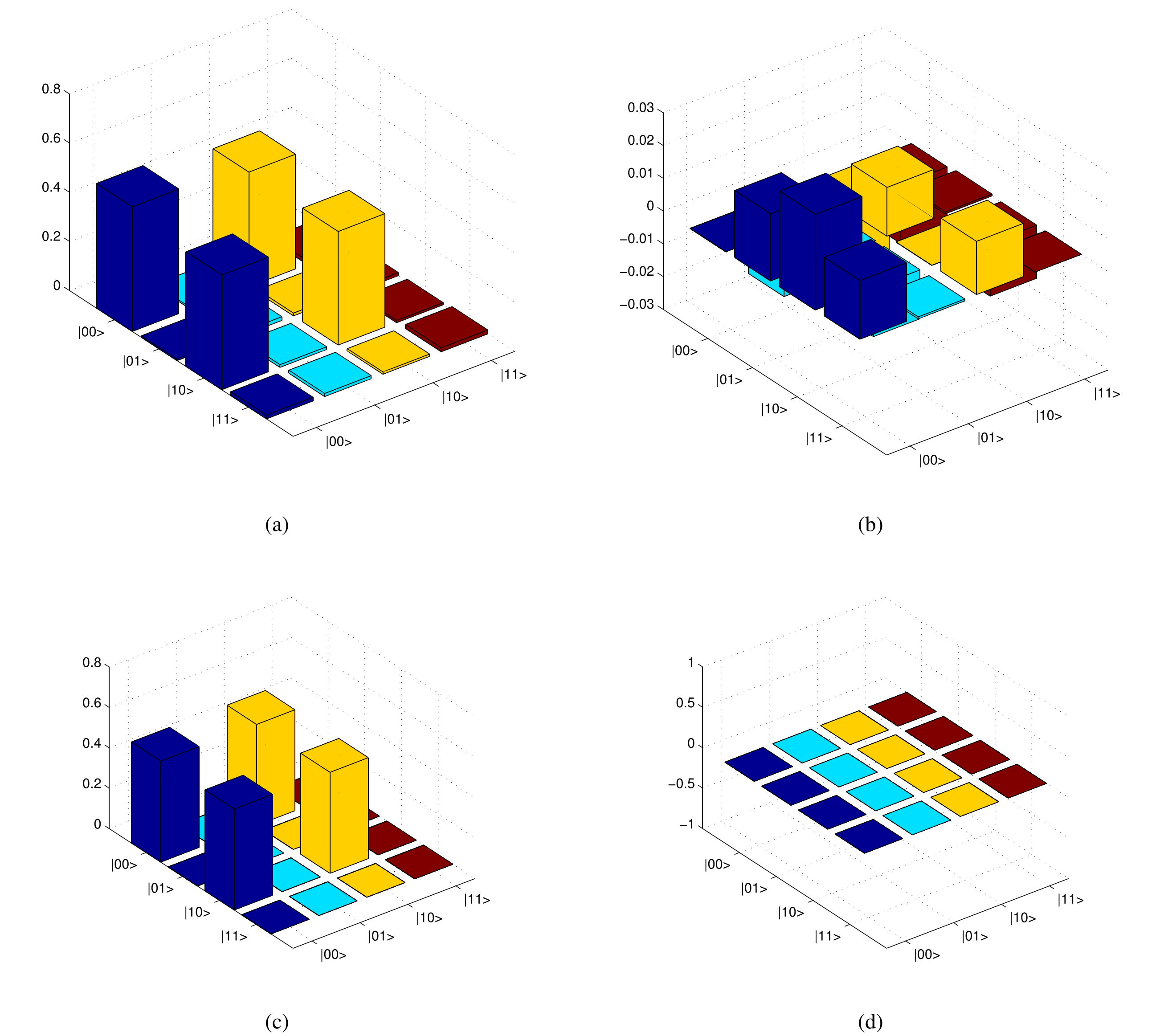

Fig. 16. State tomography results of the $|td\rangle$ qubits. The first row shows the real (a) and the imaginary (b) parts of the experimentally reconstructed density matrix ρ^{Ex}, while the second row shows the real (c) and the imaginary (d) parts of the theoretical density matrix ρ^{Th} when the Boolean function f_0 is applied on the qubit $\frac{|0\rangle+|1\rangle}{\sqrt{2}}$.

Experimental realization of the proposed algorithm using IBM's quantum computer

In this section, the proposed algorithm is realized experimentally using IBM's 5-qubit quantum computer. To realize the proposed algorithm, we need to implement three main parts: unknown qubit $|t\rangle$ generator, the oracle U_f that represents each of the four different Boolean functions which can be generated from uni-variate Boolean function and the concurrence measurement operator D. For implementing the first part, following [54], it is assumed that the state of $|t\rangle$ is known to the preparation operator, but unknown to anybody else. Consequently, in this experiments, the state of the qubit of $|t\rangle$ is prepared in three different states as:

$$|t\rangle = \sqrt{\frac{1}{4}}|0\rangle + \sqrt{\frac{3}{4}}|1\rangle, \quad |t\rangle = \sqrt{\frac{1}{3}}|0\rangle + \sqrt{\frac{2}{3}}|1\rangle \quad and \quad |t\rangle = \sqrt{\frac{1}{2}}|0\rangle + \sqrt{\frac{1}{2}}|1\rangle. \tag{23}$$

Secondly, U_f is implemented as four different circuits, shown in Fig. 2, to be applied (to each) (on the) unknown qubit $|t\rangle$. Finally, although we have defined that the physical concurrence measurement is a black box operator D, in this section for experimental realization purposes, this black-box will be implemented using Romero et al. protocol [45].

Implementation of the proposed algorithm at real IBM QC

Four experiments are conducted using ibmqx4 chip for each unknown qubit $|t\rangle$ described by Eq. (23). In each experiment, the oracle U_f is implemented by one of the four cases shown in Fig. 2. Three decoupled replicas of each circuit shown in Fig. (2) are used to conduct each experiment on IBM's real quantum computer. Two of these replicas are fed to the concurrence measurement protocol (see Fig. 3) which explained in Section 'Concurrence measurement realization' to measure the concurrence according to step 3 in the proposed algorithm (see Section 'The proposed algorithm'). We ran each experiment 10 times and calculated the standard deviation of the data obtained for each case. The number of times that the measurements are conducted on the

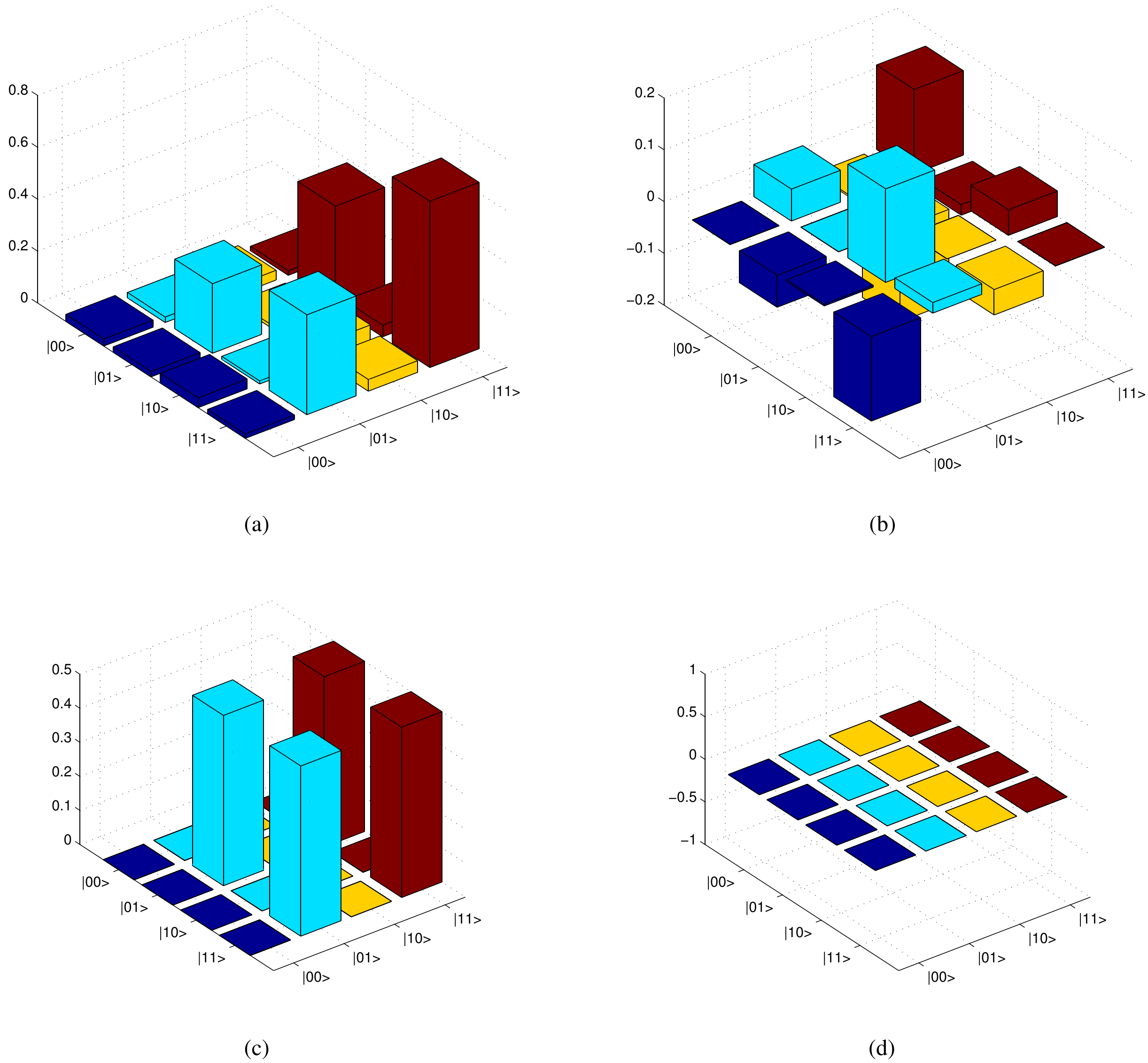

Fig. 17. State tomography results of the $|td\rangle$ qubits. The first row shows the real (a) and the imaginary (b) parts of the experimentally reconstructed density matrix ρ^{Ex}, while the second row shows the real (c) and the imaginary (d) parts of the theoretical density matrix ρ^{Th} when the Boolean function f_1 is applied on the qubit $\frac{|0\rangle+|1\rangle}{\sqrt{2}}$.

experiment circuit is called the number of shots. It is worth mentioning to note that each run is executed with 8192 shots.

Results and discussion

The experiment results, with standard deviation, compared with the theoretical results are plotted as bar charts as shown in the Fig. 4–15. The red histograms represent the theoretical results whereas the blue ones represent experimental results. The green ones represent simulation results, the simulation experiments are performed via $ibmq_{qasm_{simulator}}$. The bar charts shown from Fig. 4–15 correspond to the four Boolean functions, respectively, when applied on the unknown qubit $|t\rangle$. Fig. 4–7 show the bar charts when applied the four Boolean functions on $|t\rangle = \sqrt{\frac{1}{4}}|0\rangle + \sqrt{\frac{3}{4}}|1\rangle$. However, Fig. 4–8 show the bar charts when applied the four experiments on $|t\rangle = \sqrt{\frac{1}{3}}|0\rangle + \sqrt{\frac{2}{3}}|1\rangle$. Finally, Fig. 12–15 illustrate the bar charts when applied on the unknown qubit $|t\rangle = \sqrt{\frac{1}{2}}|0\rangle + \sqrt{\frac{1}{2}}|1\rangle$. Each of those figures shows the count number each different state of Eq. (5) can take from the concurrence measurement circuit (shown in Fig. (3)). The statistical fidelities for the circuit used to realize the proposed algorithm, shown in Fig. (3)) are reported in Tables 2 and 3. The statistical fidelities have been calculated according to $F = \sum_{k=0}^{2^n-1}\sqrt{p_k^{Ex}p_k^{Th}}$ (where n is the number of qubits and p_k^{Ex}, p_k^{Th} are the experimental and theoretical probabilities, respectively, for the k^{th} state [21]).

In the conducted experiments, three main remarks are reported, first: in Romero et al. circuit, the concurrence can be quantified, experimentally, through determination of the probability of state $|0000\rangle$ or probability of state $|1010\rangle$ in Eq. (6). Concretely, Romero et al. [45] chose to quantify the probability of state $|0000\rangle$ to realize their protocol

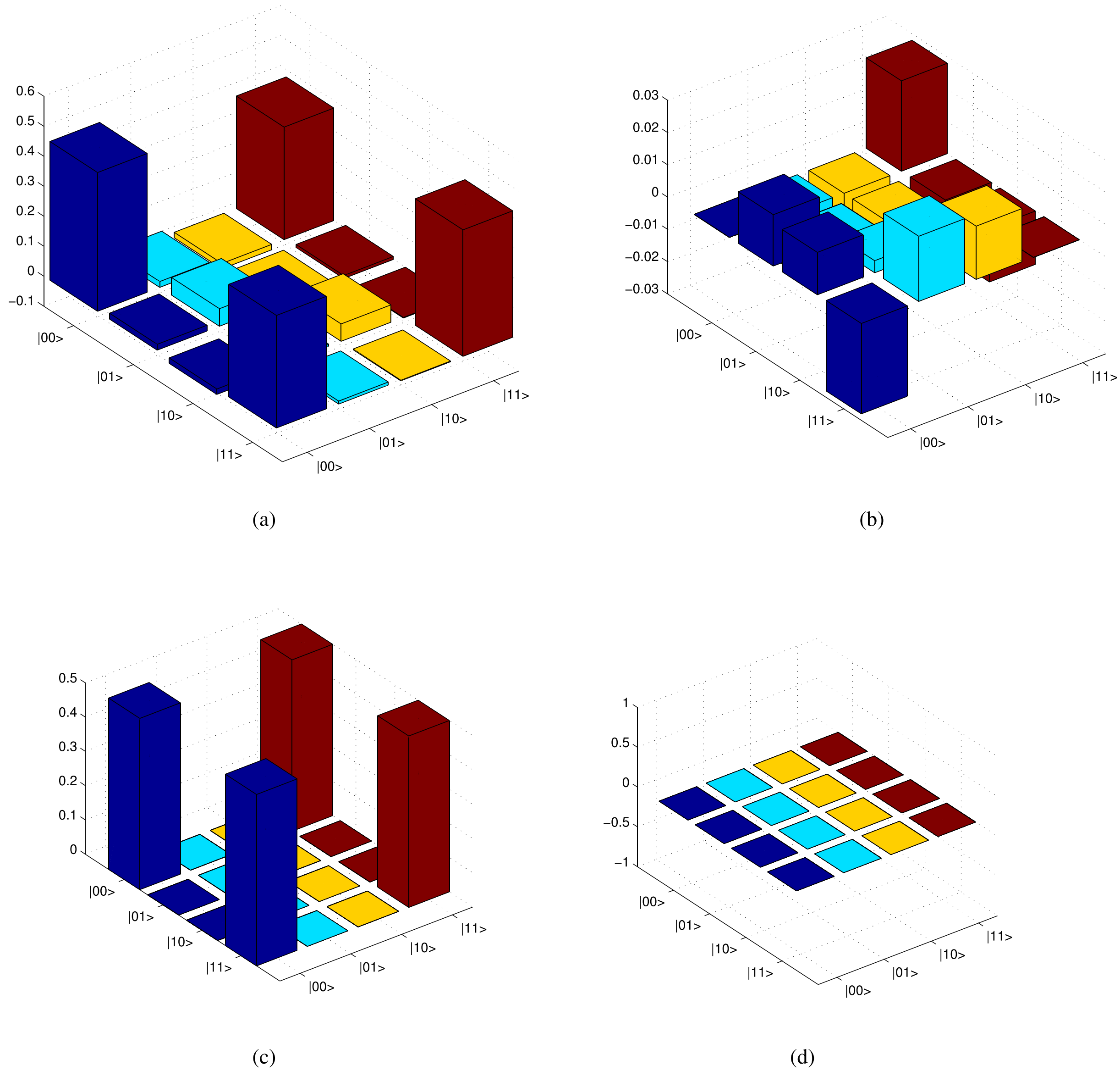

Fig. 18. State tomography results of the $|td\rangle$ qubits. The first row shows the real (a) and the imaginary (b) parts of the experimentally reconstructed density matrix ρ^{Ex}, while the second row shows the real (c) and the imaginary (d) parts of the theoretical density matrix ρ^{Th} when the Boolean function f_2 is applied on the qubit $\frac{|0\rangle+|1\rangle}{\sqrt{2}}$.

physically using the two scenarios mentioned in Section 'Concurrence measurement realization'. However, the bar charts shown in the figures shown from Fig. 4–15 is a physical realization of this circuit using IBMs 5-qubit quantum computer. It is evident from the bar charts plotted in the figures shown in Figs. 4, 5, 8, 9, 12 and 13 that the probability of state $|1010\rangle$ is more accurate to quantify the concurrence in contrast with the probability of the state $|0000\rangle$ when the concurrence between the qubits $|t\rangle$ and $|d\rangle$ is vanished ($C = 0$). Conversely, the probability of state $|0000\rangle$ is more accurate compared with the probability of the state $|1010\rangle$ when the concurrence is emphasized ($C > 0$) between the same qubits as depicted from the bar charts plotted in the figures shown in Figs. 6, 7, 10, 11, 14 and 15. So, we can figure out that both probabilities of the states $|1010\rangle$ and $|0000\rangle$ are considered together in order to quantify the concurrence more precisely between the qubits $|t\rangle$ and $|d\rangle$ experimentally. Secondly, it is evident from the bar charts plotted in the figures shown in Figs. 4, 5, 8, 9, 12 and 13 that the concurrence value for constant functions, f_0 and f_1, is negligible experimentally especially when considering the probability of the state $|1010\rangle$. On the other hand, the concurrence value is considered significantly for balanced functions, f_2 and f_3, as obvious in the probability of state $|0000\rangle$ shown in Figs. 6, 7, 10, 11, 14 and 15 and that matches the prediction of the proposed algorithm again.

Third, it is obvious from the simulation results, plotted by green bars, in Figs. 4, 5, 8, 9, 12 and 13 that the probabilities of the states $|0000\rangle$ and $|1010\rangle$, are matched typically theoretical results. Whereas both of them predicts that concurrence value is $C = 0$ according to Eq. (6) for constant functions. Also, it is depicted from Figs. 6, 7, 10, 11, 14 and 15 that the probabilities of the states $|0000\rangle$ and $|1010\rangle$ of the simulation results match the theoretical results approximately for measuring that concurrence value as $C > 0$ for balanced functions. Fourth, Tables 2–4 shows the comparison between the theoretical value of $|\alpha|$ the estimated value of $|\alpha|$ obtained by simulation results and real quantum computer. The negligible difference between the theoretical results and simulation results is due to that the number of shots is 8192. These results will be matched exactly, which is not important, when the number of measurements (shots) is infinity. However, this negligible difference has no effect absolutely about the result of the proposed algorithm according to the figures Fig. 4–15. The gap between theoretical results and the

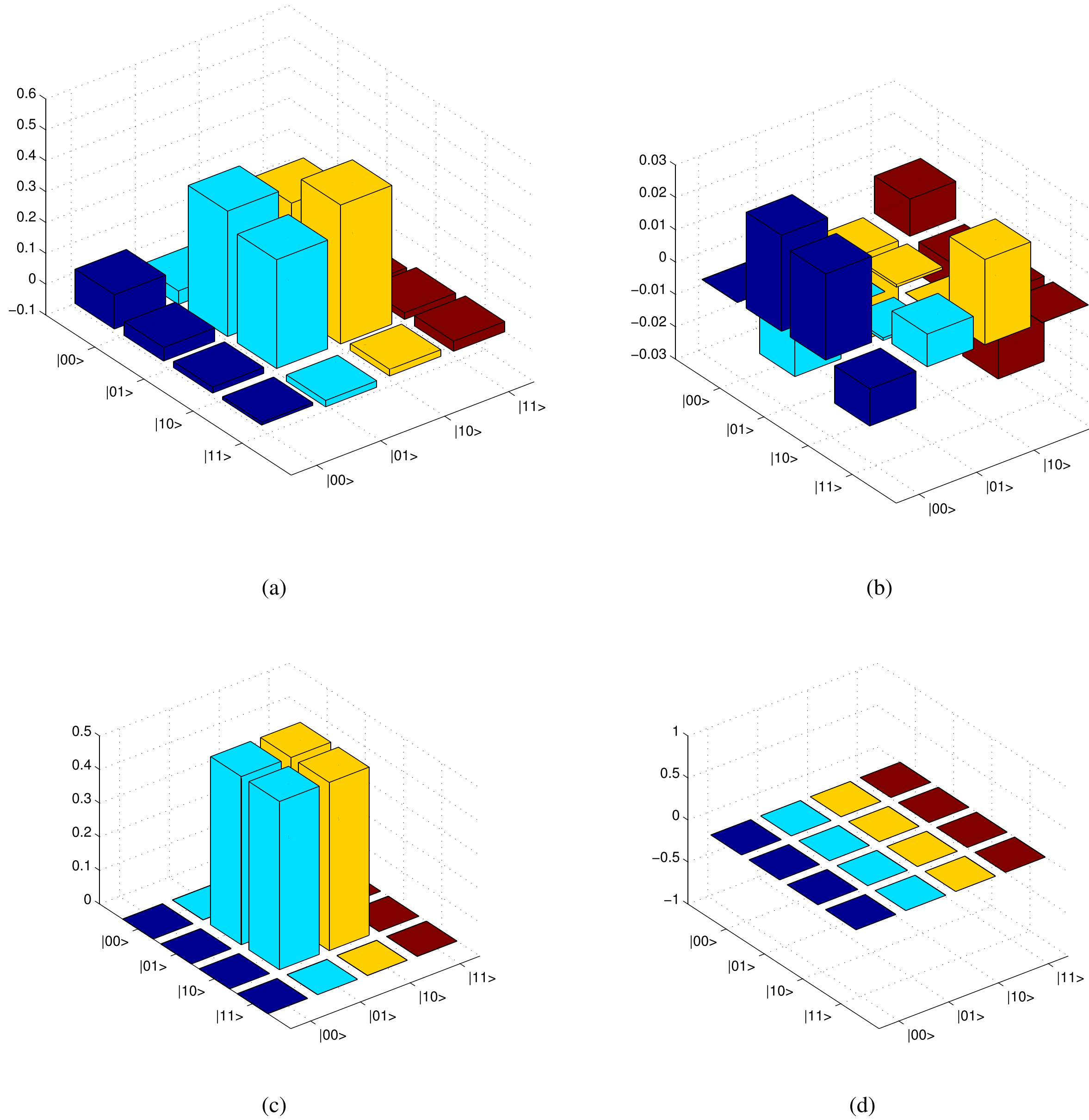

Fig. 19. State tomography results of the $|td\rangle$ qubits. The first row shows the real (a) and the imaginary (b) parts of the experimentally reconstructed density matrix ρ^{Ex} , while the second row shows the real (c) and the imaginary (d) parts of the theoretical density matrix ρ^{Th} when the Boolean function f_3 is applied on the qubit $\frac{|0\rangle+|1\rangle}{\sqrt{2}}$.

experimental results of realizing the proposed algorithm on real IBM's quantum computer, ibmqx4, is owing back to built-in errors combined with ibmqx4 chip. The qubits and the gates in ibmqx4 chip have some fixed value of errors. The architecture of the chip ibmqx4 used in the experiments is shown in Table 5 with the associated errors. Finally, it is lucid from Table 1 that the experimental results of realizing the proposed algorithm on real IBM's quantum computer, ibmqx4, when tested on different values of the unknown qubit $|t\rangle$ with high fidelities. The general trend of decrease in fidelity is when moving from left to right in Table 1, the highest fidelities being for f_0-is attributable to the fact that the number of gates in a circuit increases for circuits f_0 up to f_3.

Experimental realization of the analysis of the proposed algorithm via quantum state tomography

The analysis of the proposed algorithm is explained in Section 'Analysis of performance'. To prove our analysis experimentally, quantum state tomography (QST) is the most reliable method used for reconstructing the quantum state from an experimental source [55–58]. In QST, the experimental density matrix ρ^{Ex} is calculated based on set of measurements and compared with the theoretical density matrix ρ^{Th}. Here additional experiment is conducted, whereas the state of the qubit $|t\rangle$ is $\sqrt{\frac{1}{2}}|0\rangle + \sqrt{\frac{1}{2}}|1\rangle$. The experiment conducted four times such that in each time one of the four possible Boolean functions, f_0, f_1, f_2 and f_3, is applied and then the experimental and the theoretical density matrices are calculated and plotted. In each experiment, three measurements performed in the x, y, and z-basis with 8192 shots. The default measurement in IBM's quantum computer is in the direction of z-axis basis. However, to perform measurement operation on a qubit in the x-axis, the Hadamard-gate H is applied on that qubit before measurement process. Also, the application of $S^{\dagger}$ followed by H gates before the measurement process is equivalent to measurement in the direction of the y-axis. Then the experimental density matrix of the two-qubit system is calculated [59,60] as:

$$\rho^{Ex} = \frac{1}{4}\sum_{j_1,j_2=0}^{3} M_{j_1 j_2}(\sigma_{j_1} \otimes \sigma_{j_2}). \tag{24}$$

Since the 16 coefficients $M_{j_1 j_2}$ are real numbers [59] and require only 9 measurements to be estimated [59,61]. where σ_{j_i} represents the Pauli-gates [21], I, X, Y and Z, applying on the i^{th} qubit. The theoretical density matrix is caluclated from $\rho^{Th} = |td\rangle^{Th}\langle td|^{Th}$. The state of $|td\rangle^{Th}$ is described by Eqs. (7), (10), (13) and (16) which are corresponds to the Boolean functions f_0, f_1, f_2 and f_3, respectively. The experimental and theoretical matrices corresponds to the four Boolean functions are shown in Fig. 16–19, respectively. The distance between theoretical density matrix and experimental density matrix of quantum states is measured by the fidelity which is defined as

$$F(\rho^{Ex}, \rho^{Th}) = Tr\left(\sqrt{\sqrt{\rho^{Th}}\,\rho^{Ex}\sqrt{\rho^{Th}}}\right)$$

The fidelities of this experiment is calculated as 0.95, 0.84,0.82, 0.78 corresponds to f_0 f_1, f_2 and f_3, respectively. Again, the gap between theoretical and experimental density matrices is due to the built-in errors combined with ibmqx4 chip as reported in Table 5. The overlap between the two density matrices shows how close the theoretical and experimental quantum states and proves the analysis explained in Section 'Analysis of performance'.

Conclusion

This paper shows the ability to integrate entanglement measurement, concretely concurrence, as a crucial ingredient, with quantum parallelism and interference to solve a generalized version of Deutsch's problem. The proposed algorithm classifies whether an orcale U_f, when applied on an unknown qubit $|t\rangle = \alpha|0\rangle + \beta|1\rangle$, is constant or balanced Boolean function and also recognizes concretely which function is applied among the four possible Boolean functions via this oracle. The proposed algorithm is tested experimentally using IBMs 5-qubit quantum computer (ibmqx4). The obtained results realized the proposed algorithm with high fidelity. The analysis of the proposed algorithm is also verified through quantum state tomography.

Declaration of Competing Interest

The authors declare that they have no known competing financial interests or personal relationships that could have appeared to influence the work reported in this paper.

References

[1] Riedinger R, Marinković I, Löschnauer C, Aspelmeyer M, Hong S, Wallucks A, Gröblacher S. Remote quantum entanglement between two micromechanical oscillators. Nature 2018;556:473–7.
[2] Hennessy K, Winger M, Gerace D, Atatüre M, Gulde S, Fält S, Hu EL, Imamoğlu A, Badolato A. Quantum nature of a strongly coupled single quantum dotcavity system. Nature 2007;445:896–9.
[3] Modi K, Son W, Vedral V, Paterek T, Williamson M. Unified view of quantum and classical correlations. Phys Rev Lett 2010;104:080501.
[4] Kampel NS, Fischer R, Yu PL, Cicak K, Simmonds R, Lehnert K, Peterson RW, Regal C. Improving broadband displacement detection with quantum correlations. Phys Rev X 2017;7:021008. doi: https://doi.org/10.1103/PhysRevX.7.021008.
[5] Xu JS, Li CF, Zhang C-J, Zou X-B, Xu XY, Guo GC. Experimental investigation of classical and quantum correlations under decoherence. Nat Commun 2010;1:7.
[6] Oreshkov O, Costa F, Brukner C. Quantum correlations with no causal order. Nat Commun 2012;3:1092.
[7] Sainz AB, Acín A, Guryanova Y, Navascués M. Almost-quantum correlations violate the no-restriction hypothesis. Phys Rev Lett 2018;120:200402.
[8] Sete EA, Rostovtsev YV, Eleuch H, Jha PK, Svidzinsky AA, Sucke S. Using quantum coherence to generate gain in the xuv and x-ray: Gain-swept superradiance and lasing without inversion. IEEE J Select Top Quant Electr 2012;18(1):541–53.
[9] Jha PK, Eleuch H, Rostovtsev YV. Coherent control of atomic excitation using off-resonant strong few-cycle pulses. Phys Rev A 2010;82(4):045805.
[10] Eleuch H, Rotter I. Resonances in open quantum systems. Phys Rev A 2017;95(2). 022117.
[11] Eleuch H, Rotter I. Open quantum systems and dicke superradiance. Eur Phys J D 2014;68(3):74.
[12] Mohamed AB, Eleuch H. Non-classical effects in cavity qed containing a nonlinear optical medium and a quantum well: entanglement and non-gaussanity. Eur Phys J D 2015;69(8):191.
[13] Berrada K, Eleuch H, Abdel-Khalek S, Hassouni Y. Beam splitting and entanglement generation: excited coherent states. Quant Inform Process 2013;12(1):69–82.
[14] Reid MD, Drummond PD. Quantum correlations of phase in nondegenerate parametric oscillation. Phys Rev Lett 1988;60:2731.
[15] Lu CY, Gühne O, Gao WB, Zhang J, Yuan ZS, Goebel A. Yang T, Zhou XQ, Pan JW. Experimental entanglement of six photons in graph states. Nat Phys 2007;3(2):91.
[16] Abdel-Aty M. Delayed sudden birth and sudden death of entanglement in josephson-charge qubits. Laser Phys 2009;19(2):511.
[17] Li M, Fei SM, Zhao MJ, Wang ZX. Experimental detection of quantum entanglement. Front Phys 2013;8(4):357.
[18] Zhang LH, Yang M, Cao ZL. Direct measurement of the concurrence for two-photon polarization entangled pure states by parity-check measurements. Phys Lett A 2013;377:1421–4.
[19] Regula B, Adesso G. Entanglement quantification made easy: polynomial measures invariant under convex decomposition. Phys Rev Lett 2016;116. 070504.
[20] Gühne O, Tòth G. Entanglement detection. Phys Rep 2009;474(1):1–75.
[21] Nielsen MA, Chuang IL. Quantum computation and quantum information. Cambridge, England: Cambridge University Press, vol. 20; 2000. p. 317–30.
[22] Einstein A, Podolsky B, Rosen N. Can quantum-mechanical description of physical reality be considered complete? Phys Rev 1935;47(10):777. doi: 10.1007/s12110-009-9068-2.
[23] Freedman SJ, Clauser JF. Experimental tests of realistic local theories via bell's theorem. Phys Rev Lett 1972;28:938.
[24] Aspect A, Grangier P, Roger G. Experimental tests of realistic local theories via bell's theorem. Phys Rev Lett 1981;47:460.
[25] Aspect A, Grangier P, Roger G. Experimental realization of einstein-podolsky-rosen-bohm gedankenexperiment: a new violation of bell's inequalities. Phys Rev Lett 1982;49:938.
[26] Bose S, Plenio MB, Knight PL, Vedral V. Proposal for teleportation of an atomic state via cavity decay. Phys Rev Lett 1999;83:5158.
[27] Gordon G, Rigolin G. Generalized teleportation protocol. Phys Rev A 2006;73. 042309.
[28] Wootters WK. Entanglement of formation of an arbitrary state of two qubits. Phys Rev Lett 1998;80:2245.
[29] Zidan M. A novel quantum computing model based on entanglement degree. Mod Phys Lett B 2020;34(35):2050401.
[30] Deutsch D. Quantum theory, the church-turing principle and the universal quantum computer. Proc R Soc Lond A 1985;400:97.
[31] Deutsch D, Jozsa R. Rapid solution of problems by quantum computation. Proc R Soc Lond A 1992;439:553.
[32] Grover LK. Quantum mechanics helps in searching for a needle in a haystack. Phys Rev Lett 1997;79(2):325.
[33] Shor P. Polynomial-time algorithms for prime factorization and discrete logarithms on a quantum computer. SIAM J Comput 1997;26(5):1484.
[34] Lesovik GB, Suslov MV, Lebedev AV, Sadovskyy IA, Vinokur VM. Arrow of time and its reversal on the ibm quantum computer. Sci Rep 2019;9:4396.
[35] Bennett CH, Crépeau C, Jozsa R, Peres A, Brassard G, Wootters WK. Teleporting an unknown quantum state via dual classical and einstein-podolsky-rosen channels. Phys Rev Lett 1993;70:1895.
[36] Zhang Q, Wagenknecht C, Chen YA, Zhao B, Yang T, Mair A, Schmiedmayer J, Goebel A, Pan JW. Experimental quantum teleportation of a two-qubit composite system. Nat Phys 2006;2:678–82.
[37] Chou KS, Wang CS, Reinhold PC, Axline CJ, Gao YY, Frunzio L, Devoret MH, Jiang L, Blumoff JZ, Schoelkopf RJ. Deterministic teleportation of a quantum gate between two logical qubits. Nature 2018;561:368–73. doi: https://doi.org/10.1038/s41586-018-0470-y.
[38] Nagata K, Nakamura T. Generalization of deutsch's algorithm. Int J Theor Phys 2020;59:2557–61. doi: https://doi.org/10.1007/s10773-020-04522-0.
[39] Mintert F, Kus M, Carvoalho ARR, Buchleitner A. Measures and dynamics of entangled states. Phys Rep 2005;415:207.
[40] Mintert F, Kus M, Carvoalho ARR, Buchleitner A. Assortative pairing and life history strategy – a cross-cultural study. Phys Rev Lett 2005;95:260502.
[41] Walborn SP, Davidovich L, Mintert F, souto Ribeior PH, Buchleitner A. Experimental determination of entanglement with a single measurement. Nature 2006;440:1022.
[42] Walborn SP, Davidovich L, Mintert F, Souto Ribeiro PH, Buchleitner A. Experimental determination of entanglement by a projective measurement. Phys Rev A 2007;75:032338, doi: https://doi.org/10.1103/PhysRevA.75.032338.
[43] Horodecki P. Measuring quantum entanglement without prior state reconstruction. Phys Rev Lett 2003;90. 167901.
[44] Zhang LH, Yang M, Song W, Yang Q, Cao ZL. Direct measurement of the concurrence of two-photon polarization-entangled states. Phys Rev A 2013;88: 062342.
[45] Romero G, Lastra F, Solano E, López CE, Retamal JC. Direct measurement of concurrence for atomic two-qubit pure states. Phys Rev A 2007;75:032303.
[46] Chen L, Zhang LH, Yang M, Cao ZL. Directly measuring the concurrence of two-atom state via detecting coherent lights. Laser Phys Lett 2017;14(11):115205.
[47] Zhang LH, Yang M, Cao ZL. Direct measurement of the concurrence for two-photon polarization entangled pure states by parity-check measurements. Phys Lett A 2013;377:1421–4, doi: https://doi.org/10.1016/j.physleta.2013.04.018.

[48] Zhou L. Measurement of arbitrary two-photon entanglement state with the photonic faraday rotation. arXiv:1401.6719 (2014).
[49] Lee SM, Lee S-B, Ji S-W, Zubairy MS. Proposal for direct measurement of concurrence via visibility in a cavity qed system. Phys Rev A 2008;77:040301, doi: https://doi.org/10.1103/PhysRevA.77.040301.
[50] Zhou L, Sheng YB. Detection of nonlocal atomic entanglement assisted by single photons. Phys Rev A 2014;90. https://doi.org/10.1103/PhysRevA.90.024301. 024301.
[51] Sheng YB, Pan J, Zhou L, Gu R, Wang XF. Two-step measurement of the concurrence for hyperentangled state. Quantum Inf Process 2015;14:963–78.
[52] Tukiainen M, Kobayashi H, Shikano Y. Quantification of concurrence via weak measurement. Phys Rev A 2017;95:052301.
[53] Zhou L, Sheng YB. Concurrence measurement for the two-qubit optical and atomic states. Entropy 2015;17:4293.
[54] Behera BK, Banerjee A, Panigrahi PK. Experimental realization of quantum cheque using a five-qubit quantum computer. Quantum Inf Process 2017;16:312.
[55] Vogel K, Risken H. Determination of quasiprobability distributions in terms of probability distributions for the rotated quadrature phase. Phys Rev A 1989;40:2847.
[56] Leonhardt U. Quantum-state tomography and discrete wigner function. Phys Rev Lett 1995;74:4101–5.
[57] White AG, Eberhard PH, James DFV, Kwiat PG. Nonmaximally entangled states: production, characterization, and utilization. Phys Rev Lett 1999;83:3103–7.
[58] Titchener JG, Heilmann R, Solntsev AS, Szameit A, Gräfe M, Sukhorukov AA. Scalable on-chip quantum state tomography. npj Quantum Inf 2018;4:19, doi: https://doi.org/10.1038/s41534-018-0063-5.
[59] James DFV, Munro WJ, Kwiat PG, White AG. Measurement of qubits. Phys Rev A 2001;64:052312.
[60] Vishnu PK, Behera KB, Joy D, Panigrahi PK. Experimental demonstration of non-local controlled-unitary quantum gates using a five-qubit quantum compute. Quant Inf Process 2018;17:1:17. doi: https://doi.org/10.1007/s11128-018-2051-2.
[61] Figueredo AJ, Wolf PSA. Assortative pairing and life history strategy – a cross-cultural study. Human Nat 2009;20:317–30.